Integrated geophysical and sedimentological datasets for assessment of offshore borrow areas: the CHIMERA project (western Portuguese Coast)

Mário Mil-Homens[1]*, Pedro Brito[2,4,6], Vitor Magalhães[2,6], Marcos Rosa[2], Marta Neres[2,6], Marta Silva[4], Emília Salgueiro[2,3], Teresa Drago[2,6], Ana Isabel Rodrigues[1], Miriam Tuaty Guerra[1], Maria José Gaudêncio[1], Eveline Almeida[4], Mariana Silva[4], Mafalda Freitas[2], Celso Aleixo Pinto[5], Cidália Bandarra[1] and Pedro Terrinha[2,6]

[1]Divisão de Oceanografia e Ambiente Marinho, Instituto Português do Mar e da Atmosfera, I.P., Rua Alfredo Magalhães Ramalho, 6, 1495-006 Lisboa, Portugal

[2]Divisão de Geologia e Georrecursos Marinhos, Instituto Português do Mar e da Atmosfera, I.P., Rua C ao Aeroporto, 1749-077 Lisboa, Portugal

[3]CCMAR – Centre of Marine Sciences, Universidade do Algarve, Faro, 8005-139, Portugal

[4]Xavisub – Mergulhadores Profissionais, LDA. Rua José Silva Mariano, 3830-688, Gafanha da Nazaré - Ílhavo, Aveiro, Portugal

[5]Núcleo de Monitorização Costeira e Risco, Departamento do Litoral e Proteção Costeira, Agência Portuguesa do Ambiente, Rua da Murgueira, 9/9A Zambujal, Ap. 7585, 2610-124 Amadora, Portugal

[6]Instituto Dom Luiz (IDL), Faculdade de Ciências da Universidade de Lisboa, Campo Grande Edifício C1, Piso 1, 1749-016 Lisboa, Portugal

MM-H, 0000-0002-1570-2641; VM, 0000-0002-3205-771X; MN, 0000-0003-3939-4636; TD, 0000-0003-3496-3270; MTG, 0000-0003-0178-310X; MJG, 0000-0002-6303-9995; EA, 0000-0001-8769-4583; MF, 0000-0002-9953-4146; PT, 0000-0002-6824-6002

*Correspondence: mario.milhomens@ipma.pt

Abstract: Coastal erosion impact on low-lying sandy shorelines represents a worldwide problem, which is particularly felt in various segments of the Portuguese coast where this geomorphological type represents 42% of its total length. Beach nourishment is a viable engineering alternative for shore protection and the assessment of offshore sources of beach-fill material is an essential aspect when implementing this mitigation strategy. The CHIMERA project carried out a multidisciplinary inspection on four segments of the west Portuguese coast to assess their potential as offshore borrow areas for beach nourishment. Altogether, these segments covered an area of *c.* 35 km^2, at water depths between 20 and 42 m. They were surveyed using multibeam, sub-bottom profiler, ultra-high resolution multichannel seismics and a set of 126 surface samples and 72 vibrocores (with 3 m long each). To comply with the Portuguese legislation, sand types were assessed by granulometric and chemical analyses for evaluating the quality of sediments in terms of contamination. High-resolution magnetic surveys were conducted to find potential archaeological artefacts. The adopted methodology proved to be adequate to quantify and describe the spatial distribution of useful sediment volumes, supporting the ongoing Integrated Coastal Sediment Strategy for mainland Portugal.

Supplementary material: Classification of sediment's quality according to the Portuguese legislation (Ordinance 1450/2007) in the FFLV area is available at https://doi.org/10.6084/m9.figshare.c.5007266

Portugal has a shoreline 987 km long, geomorphologically dominated by low-lying sandy beaches (42%), rocky cliffs (48%), soft cliffs (2%) and low-lying rocky coast (8%). Sandy beaches have always attracted humans and human activities, having an important economic, social and recreational value. However, in some areas, beaches are becoming extremely vulnerable and at risk of disappearance. Besides that, beaches are important natural barriers that provide improved protection to upland structures and infrastructure from the effect of storms. The Portuguese coast is undergoing environmental pressures caused by the increase of the population density (major Portuguese cities are located along the coast), by the expansion of the construction of heavy infrastructures (e.g. harbours) and of coastal hard

From: Asch, K., Kitazato, H. and Vallius, H. (eds) *From Continental Shelf to Slope: Mapping the Oceanic Realm.* Geological Society, London, Special Publications, **505**, https://doi.org/10.1144/SP505-2019-100

engineering structures (e.g. groins and revetments behind the jetties), and by the growing of touristic maritime activities. Some sectors of the Portuguese western coast, particularly sandy beaches and soft rock cliffs are affected by the increase in the rates of coastal erosion. The present-day negative sedimentary budget of the Portuguese coast result in a generalized retreat of the coastline (Andrade *et al.* 2015) along approximately 20% of its total length. According to Ferreira and Matias (2013), three main causes contribute to the current coastal erosion scenario in Portugal: increasing storminess, lack in sediment supply and interventions at river basins, coastal engineering structures. These effects are being enhanced climate change, in particular, global warming. One of the main consequences of climate change relevant to the coast are sea level rise and expected changes in wave climate (i.e. increased storminess and changes in prevailing wave direction), that will generate impacts, such as increased coastal erosion and frequency and magnitude of overtopping/coastal flooding. Consequently, the protection of coastlines is a topic of growing concern for the international community (ICES 2016). Beach nourishment is an environmentally acceptable and viable engineering alternative for shore protection and restoration to mitigate coastline retreat and to preserve the socioeconomic occupation of the coast. It is used in emergency situations as a local and short-term solution (i.e. mitigation of short-term erosion induced by storms), or as a regional and long-term management strategy, that is mitigation of installed erosion tendency and vulnerability to sea-level rise (Hamm *et al.* 2002; US AID 2009). In addition to providing protection to valuable areas of the territory from an environmental and strategic point of view, artificial beach nourishment also conserves the natural state of the beach, while enhancing its recreational use. In certain situations, beach nourishment has the sole objective of improving the comfort of its users, either by increasing the area available to beach activities (Vera-Cruz 1972) or by changing the grain size of its sediments (Anthony *et al.* 2011). Beach nourishment can be assured by terrestrial sources (e.g. dredged estuarine and lagoon sediments) or by extracting marine aggregates, which have grown in importance due to the increase of land-use constraints and depletion of terrestrial aggregate resources (Van Lancker *et al.* 2017). It involves the addition of sand from an offshore borrow area to expand an eroding coastal segment, respecting the natural hydrodynamic regime. The feasibility of this type of intervention is controlled by local geomorphological (e.g. variations in the orientation of the coastline, sediment grain size), morphodynamical (e.g. long-term erosion, wave-energy magnitude, degree of beach exposure and location, length, cross-shore and long-shore sediment transport rates) and anthropogenic constraints (e.g. coastal engineering structures, beach nourishment at adjacent beaches) (Davis *et al.* 2000). However, it is important to highlight that the benefits of using marine sand and gravel for beach nourishment must be balanced with the potentially significant environmental impacts (ICES 2016).

As a result, the degree of success of a beach nourishment project varies widely and is site-specific, lasting from only a few months to several decades (Pinto *et al.* 2020). Additionally, the sand supply must fulfil the mandatory physical, chemical and environmental quality requirements of the Portuguese regulations.

To meet the requirements, detailed exploration and characterization of the source material must be done, supported by geological models based on a diverse geophysical and sampling dataset (bathymetry, reflection seismic, magnetics, sedimentology and geochemistry). This leads to an understanding of the internal variability of the aggregate deposits, not only at the seafloor, but also their variability in depth. The later requires the characterization of the borrow area in terms of their 3D geometry, physical and chemical composition, and quantification of the volume of sand and gravel that can be dredged and effectively mobilized.

The aim of the present study is to identify and to characterize (e.g. quality and quantity) the sedimentary resources on the continental shelf with a potential to be nourishing areas for future beach nourishments in adjacent coastal sectors that are eroding. This was reached through the use and integration of diverse methodological contributions to assess the sand deposits available offshore. Four case study areas along the western Portuguese inner shelf, namely Espinho-Torreira (ET), Barra-Mira (BM), Figueira da Foz-Leirosa (FF) and Costa da Caparica (CC) were selected, and their potential as sand resources (natural finite resource that must be used responsibly and appropriately to be sustainable (ICES 2016)) were evaluated. These four areas correspond to areas previously identified as potentially submitted to high-magnitude beach nourishment interventions (Andrade *et al.* 2015). These potential nourishment areas were subject to increasingly detailed surveys and studies to characterize (in terms of dimension and sedimentological characteristics) the deposit as a sand resource. This study was carried out in the context of the CHIMERA project, developed by the Portuguese Environment Agency (APA, IP) and co-funded by the POSEUR (Operational Programme for Sustainability and Efficient Use of Resources, established through an Execution Decision from the European Commission on 16 December 2014) programme (POSEUR-09-2016-48-FC-000030). The data obtained were included in an interactive spatial data infrastructure (webGIS), which provides georeferenced multi-layer cartography at a scale of the study area, using data visualization tools to be utilized as a support tool in the implementation of these proposed beach nourishment programmes.

Geological setting

The four study areas located in the north and central Portuguese continental shelf, where the sedimentary transport and deposition are the result of a complex interplay between continental and oceanic factors (Fig. 1). The sources of sediments to these study areas are the Precambrian and Paleozoic igneous and metamorphic rocks of the Variscan Belt and the Meso-Cenozoic sedimentary rocks from the Lusitanian Basin, the Mondego and the Lower Tagus Basins (Mougenot 1988). The hydrographic basins that drain and supply sediments to this part of the shelf have a temperate climate, with the rivers' discharge peaks in winter. North of about 41° N, the Douro and other rivers have large discharges and steep gradients, and because of that, much of the sediment reaches the continental shelf directly. The Portuguese coast is divided into eight cells according to its geomorphological characteristics and sedimentary dynamics (Andrade *et al.* 2002, 2015). The ET and BM are in distinct sectors of sub-cell 1b and, FF and CC borrow areas are in sub-cell 1c and cell 4 (Andrade *et al.* 2015). In the west coast, wave regime predominantly from west–NW, induce net littoral southward drift, with a potential longshore sediment transport from 1 to 2×10^6 m^3 a^{-1} (e.g. Oliveira *et al.* 1982; Vicente and Clímaco 2012). This potential transport is variable along the west coast, according to the coastline orientation, decreasing southward due to lower wave energy (Ferreira and Matias 2013). This is the main sediment transport regime adjacent to the ET, BM and FF borrow areas. South of 39° N, the fluvial transport is less vigorous, and sediments have longer residence time, especially in estuarine traps at the river mouths (such as the Tagus and Sado rivers). Adjacent to the CC borrow area, sediment dynamics is more complex due to the influence of the Tagus river ebb-delta (Taborda and Andrade 2014) with a net longshore drift towards the north in order of 10^5 m^3 a^{-1} (Taborda *et al.* 2014). The tides along the west coast are semi-diurnal and mesotidal, having the average neap tidal range of 1.0 m and average spring tidal range of 2.8 m (Ferreira and Matias 2013).

The western Portuguese continental shelf is relatively narrow and deep (Fig. 1) with an average width of about 45 km and an average shelf-break depth of 160 m (Mougenot 1988). Along the different study areas, the shelf ranges between 45 and 58 km in ET, BM and FF areas and is narrower (25 km) in the CC area. Water depths (relative to Hydrographic zero) in ET, BM, FF and CC range from 24–30, 25–34, 30–42 and 20–30 m, respectively. The shelf has, in general, a gently dipping surface. The west Portuguese shelf break is indented by several submarine canyons, notably the Nazaré canyon (located south of the FF area, Fig. 1), which nearly extends to the shore and acts as a barrier for the southward alongshore sedimentary transport, as most of the sediments are caught within the canyon head and are transported to the offshore.

The sedimentary deposits of the West Portuguese continental shelf are characterized by the dominance of sand-sized detrital grains up to 80 m MWD and biogenic carbonate grains that predominate below (Dias and Nittrouer 1984; Dias and Neal 1990). The nearshore deposits of the inner shelf, down to 30 m water depth, are dominated by well-sorted fluvial sands, that are predominantly transported southward by the dominant waves and currents. The mid-shelf, between 30 and 80 m mean water depth (MWD), is dominated by coarse sand and gravel deposits resulting from littoral processes during the Holocene transgression (Dias *et al.* 2002). The outer shelf deposits (>80 m MWD), are carbonate-rich sands with shell fragments dominating landward and finer oozes dominating seaward. The shelf break deposits (>150 m MWD) are dominated by very fine, well-sorted foraminifera sand (Dias and Nittrouer 1984). As the average sea-level was stabilized at about 3.5 ka BP (Dias *et al.* 2000) the evolution of the shelf sedimentation processes and coastline location has been essentially conditioned by the sedimentary balance (Andrade *et al.* 2015). Periods of accretion/progradation or erosion/retreat are associated with excess or deficit of sediments, leading to the migration of the coastline towards the sea or towards inland, respectively.

Material and methods

Seafloor characterization

Multibeam bathymetry and backscatter data were acquired with a Teledyne RESON T50-P multi-beam system on board of IPMA research vessels 'Noruega' and 'Diplodus'. The positioning of the vessel was controlled by an integrated system (Applanix POSMV Ocean Master) that combines the satellite positioning data received via 2 GNSS antennas and data from one inertial unit (IMU) mounted close to the multibeam transducers. During the surveys, real-time RTK corrections of the SERVIR network of CIGeoE (centimetric precisions) were used, complemented with Fugro MarineStar DGPS corrections. Navigation control was done using the Teledyne PDS2000 software. The correction for the Portuguese hydrographic vertical datum, located 2 m below the mean sea-level, was parameterized in the PDS2000 program. All depth measurements in the survey areas refer to this vertical datum.

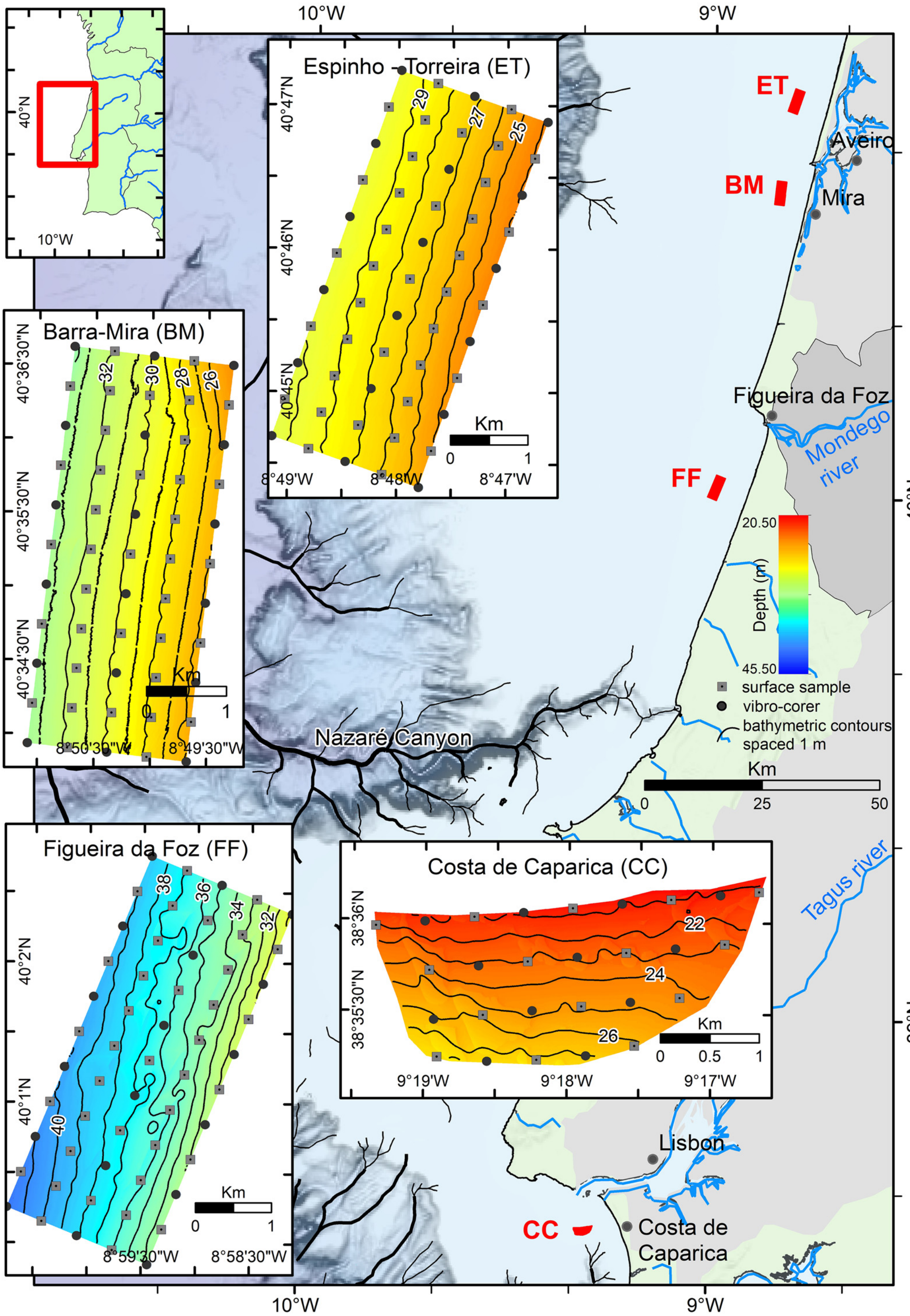

Fig. 1. Location of the four borrow areas. (**a**–**d**) Bathymetric maps for the four areas.

A Teledyne RESON T50-P multi-beam system was used for the acquisition of bathymetry and backscatter data. Sound velocity profiles were acquired during the surveys, at least twice per each survey session, using a manually deployed Odom Digibar-S SVP. The multibeam system was calibrated following standard patch test procedures.

To ensure the high resolution requested for the bathymetric survey (average resolution of 16 point/m^2), a maximum angular swath width between 110 and 100° was set, adjusted according to depth (shallower depths, greater the aperture). This parameterization maximized the acoustic signal emission rate (between 12 and 13 pulse/s) to obtain an average resolution of 25 cm along track (survey speeds between 4 and 5 kn). The resolution obtained along the swath varied between 15 and 20 cm. The main reason for the high-resolution request was to obtain a detailed seabed characterization.

The overlap between successive lines covered by the swath of the multibeam was 10% or higher. The bathymetric surveys achieved IHO Special Order specifications. The Reson T50-P multibeam system features the 'normalized snippets' functionality, which automatically normalizes the backscatter data, generating a magnitude signal compensated for the characteristics of the sonar. According to the experience already obtained in the operation of this multibeam system in former cruises made by IPMA, the frequency of 350 kHz was adopted for the acoustic signal emitted (CW) for all the surveys, allowing the acquisition of high resolution bathymetric data and backscatter data with strong signal dynamics.

Bathymetry and backscatter data processing. The navigation/position data were post-processed in POSPAC software, using the publicly available Portuguese network of GNSS base stations in order to further improve the position accuracy.

The bathymetric data was processed with Teledyne PDS2000 software. The collected SVP data was applied to each survey line, artefacts and outliers where identified and removed and the final gridded bathymetry maps (25 cm resolution) were produced. The backscatter data was processed with Fledermaus FMGeocoder Toolbox software. The processing flow included the following main steps:

- backscatter data and processed bathymetric data exported from Reson PDS files to GSF format;
- definition of sonar type and characteristics (e.g. signal frequency, beam count, gain levels);
- automatic backscatter coverage geometry calculations (using the final, corrected, bathymetry);
- automatic filtering;
- statistics calculations;
- 2 m resolution mosaic production.

Subsurface imaging

Subsurface imaging was obtained with a parametric echosounder (PE) and an ultra-high resolution multichannel seismics (UHRS). A total of about 360 km of 2D seismic lines were acquired with each system, to survey the four study areas with quadrangular 250 m spaced survey grids. The PE used was an Innomar SES-2000 Standard unit, deployed on a vessel side pole with the PE transducer and the inertial motion unit (IMU) mounted side by side at about 1.3 m below the water line. Heave compensation and roll correction based on the IMU information, were applied on-line to the seismic data. The UHRS system used was a Geo Marine Survey Systems spread, with a sparker GEO-SOURCE LW200 tips, a 1 kJ GEO-SPARK pulsed power supply and a 24 channel GEO-SENSE LW streamer with 3.125 m single element group spacing.

Seismic data processing. The implemented procedures for the seismic data processing considered two phases. The first phase consisted in the quality control (QC), carried out on-board for each line, aiming to discriminate if the acquired data qualified for further processing or if a line rerun was needed. The second processing phase carried out at the office, aimed to produce seismic sections suitable for the interpretation of the upper sedimentary layers' architecture and to identify the top of the bedrock basement.

On-board QC. The QC of the seismic data focused on assuring not only the quality of the seismic signal but also the navigation. The quality of the navigation was controlled by exporting the positioning information stored in the seismic files and overlaying it on the planed seismic lines maps. For the UHRS the vessel navigation information was integrated with the seismic spread positioning information retrieved from the source and receiver DGPS buoys. This integration resulted in filtered and smoothed navigation data, discriminating the positioning for each shot of the seismic source, the several receiver channels and the streamer feathering angle. After the navigation processing, shell scripts were used to generate plots for each line to access variations in the feathering angle, shooting interval, vessel course and tidal corrections. To control the seismic signal quality of the PE data, the ISE2 software (from Innomar) was used to apply a processing flow that comprises a noise filter, static corrections and a smoothing algorithm. To control the seismic signal quality of the UHRS data, the Deco Geophysical RadExPro software was used. The processing followed general industry standard QC procedures (e.g. Dondurur 2018) considering a flow with the following eight steps:

(1) importing of SEG-Y files and positioning data;
(2) geometry attribution and common depth point (CDP) binning;

(3) assessment of missed shots;
(4) validation of computed offsets by overlaying it with the direct arrival;
(5) assessment of the streamer depth and its nominal correction;
(6) interactive velocity analysis;
(7) band pass filter, amplitude correction, normal moveout (NMO) correction and stack;
(8) analysis of the brute stack frequency spectrum, static tidal correction and exportation of files with relevant data for further processing.

Data processing for interpretation. The seismic data processing for interpretation of both systems (PE and UHRS) was made with the software RadExPro. The processing flow applied to the UHRS data, followed the general flow proposed by Duarte *et al.* (2017). Vertical and horizontal resolutions of the datasets prepared for interpretation were assessed both graphically by minimum reflection individualization and analytically by estimation of the central frequency and the sound velocity. Estimated vertical and horizontal resolutions, sub-bottom signal penetration and other relevant characteristics of the PE non-migrated and UHRS migrated datasets prepared for interpretation are shown in Table 1.

Interpretation methodology. The aim of the seismic interpretation was twofold: (1) to establish the sedimentary architecture and to evaluate the volume of the sub-bottom uppermost unconsolidated sediment layers, and (2) to cross correlate seismic lines with vibrocores' description and evaluate volumes suitable for beach nourishment. The combined interpretation of the PE and UHRS datasets allowed the use of PE data to image and map the upper sediment layers (up to 3–5 m deep) and correlate them with the sampling data, while relying on the UHRS to image the deeper sedimentary structures until the bedrock substrate. Seismic stratigraphic interpretation was done accordingly with the general classical principles presented in Payton (1977). The number of seismic units (SU) was the minimum to ensure internal and stratigraphic coherence across each study area. Estimation of the depth and volume of the interpreted SU, were made from computation between surfaces interpolated from the picked seismic horizons, converted from two-way-time (ms) to space (m) using a mean sound spreading velocity of 1507 and 1700 ms^{-1} for the water and sediment columns, respectively.

Table 1. *Main characteristics of the interpreted PE (non-migrated) and UHRS (migrated) seismic datasets prepared for interpretation*

Characteristic	Estimated value	
	PE	UHRS
Shooting rate (Hz)	8–12	2
Sampling rate (kHz)	83	10
CDP bin (m)		1.56
Central frequency (kHz)	10	0.8–1.2
Sub-bottom penetration (m)	3–7	35–120
Vertical resolution (m)	0.04–0.25	0.1–0.5
Horizontal resolution (m)	1.7–2.9	1.6–3.2

Sediment analysis

In Portugal, sediments of borrow areas must comply with the national regulation system (Ordinance 1450/2007, 12 November) for the assessment of dredged materials that involves the determination of a set of physical and compositional parameters (grain size, organic carbon (C_{org}), total solids content and density), including contaminants (trace metals (As, Cd, Cr, Cu, Hg, Pb, Ni and Zn) and persistent organic pollutants (POPs) (hexachlorobenzene (HCB), polychlorinated biphenyls (PCBs), polycyclic aromatic hydrocarbons (PAHs))). Extracted material is classified into five categories depending on the degree of contamination: class 1, clean dredged material; class 2, slightly contaminated; class 3, moderately contaminated; class 4, contaminated; and class 5, very contaminated. These classes represent increasing concentrations on the trace metals and POPs (see Table S1 in the Supplementary material).

Sediment sampling. Surface sediment samples and cores were collected using a Van Veen grab with a sampling area of 0.1 m^2 and a vibrocoring system, respectively. The vibrocorers were recollected with the support of professional divers at the seafloor. All samples were collected in a regular mesh, spaced 0.5 km for surface samples and spaced 1 km for vibrocores, without overlap between them (Fig. 1). The sample density of surface and vibrocores is 22 and 7.2 sample/km^2, respectively.

On board, the surface samples were photographed, described, subsampled for POPs, grain size, C_{org}, density and $CaCO_3$, trace metals and total solids content. Sub-samples were stored in refrigerated conditions. Vertical cores were sectioned in 1.5 m sections, sealed and labelled. They were transported horizontally to the laboratory and maintained in refrigerated conditions until opened, described, photographed and subsampled every 25 cm for grain size and $CaCO_3$ content analyses. The archive half section of each core was stored and preserved in refrigerated conditions.

Grain-size analysis. Subsamples for grain-size analysis were dried at 100°C. Approximately 100 g of dried sample were sieved using an analytical sieve shaker (Retsch AS 200, for 2 min and at 0.9 mm of amplitude), with a set of 13 stainless-steel sieves (from 63 μm (4 phi) to 4 mm (−2 phi) with an interval of 0.5 phi). The data were processed using GRADISTAT software v 8.0 (Blott and Pye 2001). The program performs the calculation of the statistical parameters of the granulometric distribution of the sediment samples (mean grain size, standard deviation, skewness, kurtosis) using the graphical (Folk and Ward 1957) and moments (Friedman 1961) methods. Moreover, it provides the physical description of the textural group and its graphical representation in a triangular diagram, as well as the percentage distribution of the granulometric fractions of the samples according to a scale adapted from Udden (1914) and Wentworth (1922) and respective cumulative curves, allowing for the classification of the sediment types.

Density and total solids contents. The density of the sediments was determined by the ratio between the weight and the volume of the wet sediment samples (Flemming and Delafontaine 2000), corresponding to the average of the determinations in five replicates per sediment sample (results were expressed in g cm^{-3}). The content of total solids (in %), was determined by the ratio between the weight of the samples after oven drying at 100°C until reaching constant weight and their wet weight.

$CaCO_3$, C_{org} and trace metal determinations. The subsamples for the determinations of the C_{org}, $CaCO_3$ and trace metals were frozen and lyophilized. They were then sieved through a 2 mm square mesh sieve; the lower fraction was milled using agate pots in a Fritsch Pulverisette 7 Classic Line planetary mill. The $CaCO_3$ content was determined for each sample (*c.* 2.5 g) using the volumetric method (Eijkelkamp calcimeter) by measuring the CO_2 volume released by the reaction of the sample with 7 mL of HCl.

The content of C_{org} was determined using the equipment Leco Truspec micro-analyser CHNS. The content of C_{org} is calculated by the difference between total carbon content of the ground sample and the carbon content of the calcinated sample. In summary, for each ground and calcinated sample the average values of three and two readings were considered, respectively. The content of inorganic carbon was obtained by combusting the organic matter of each sample in a muffle furnace for 3 h at 400°C.

For the analysis of As, Cd, Pb, Cu, Cr, Ni and Zn, the sediments were partially decomposed by microwave (CEM Mars-XPRESS) with a mixture of HNO_3 and H_2O_2 in several steps at 95°C according to EPA method 3050B (US EPA 1996). With this methodology we intended to access the most bioavailable fraction of trace metals in the sediments. Trace metal contents were determined by induced plasma coupled mass spectrometry (ICP-MS; Thermo Elemental – X series). The elemental contents were determined by calibration curve interpolation. The limits of quantification (LQ) for this set of trace metals were obtained by regression of the points of the calibration curve. The determination of mercury (Hg) was carried out directly by thermal decomposition coupled to atomic absorption spectrometry (ET-AAS; Leco AMA 254 Mercury analyser) (Costley *et al.* 2000). The LQ for Hg was obtained considering the ratio between the sum of the average value of the blank reads and ten times the standard deviation of the readings of the blanks and the average mass of the sediment used. QC was ensured by blank analysis, certified reference material (CRM) MESS-3 (National Research Council of Canada) and duplicate samples that underwent the same type of preparation of the remaining samples. Blank samples were used to infer contamination during the analytical procedure, whereas the CRM and the duplicates allowed to evaluate the accuracy and precision of the analytical methodology used.

POPs analyses. The sub-sample for POP determinations were dried at 40°C. POPs were extracted using the ASE equipment (Dionex, ASE 200 Accelerated Solvent Extraction) with dichloromethane/hexane (1:1, v/v) at 100°C and 1500 psi; two cycles of 5 min. The following polycyclic aromatic hydrocarbon (PAHs) compounds were quantified: benzo(a)-pyrene (BaP), benzo(ghi)pyrene, indeno(1,2,3-cd) pyrene (InP), benzo[b]fluoranthene (BbF), benzo[k] fluoranthene (BkF), benzo(ghi)-perylene (BgP), anthracene (A), benzo[a]anthracene (BaA), phenanthrene (Phe), fluoranthene (Flu), pyrene (Pyr), chrysene (Chr) and naphthalene (N). For PAHs quantification, extracts were first treated with metallic copper for *c.* 12 h, then purified by column chromatography on silica/alumina (1:1), eluting with hexane and 9:1 and 4:1 hexane/dichloromethane mixtures. Then they were concentrated and injected into a gas chromatograph (Thermo, Trace GC ultra) coupled to a mass spectrometer operating in SIM mode (Selected Ion Monitoring mode) using a DB-5 capillary column (30 m × 0.25 mm, 0.25 mm). Compounds were identified by comparison of the retention times and the mass-to-charge ratio (m/z) of the compounds with those of a NIST-PAH standard solution (SRM 2260a) containing the same analytes. The quantification was performed using calibration lines with at least nine concentrations of that standard solution. For the quantification of PCBs (congeners CB26, CB52, CB118, CB118, CB138, CB153 and CB180) and HCB, the crude extracts were purified by column chromatography using Florisil as the solid phase, eluting with 15 ml of hexane (fraction I – PCBs) and 45 ml of hexane/dichloromethane

(70:30) (fraction II – HCB). The two fractions were treated with H_2SO_4 for about 12 h, then the purified extracts were concentrated under nitrogen flow and injected into a gas phase chromatograph (Agilent Technologies, 6890N network GC system) equipped with an electron capture detector (micro-ECD) Agilent Technologies, with a DB-5 capillary column (60 m × 0.25 mm, 0.25 µm) and an auto sampler. The quantification of the various compounds was carried out using calibration lines and the external standard method.

Magnetics

Magnetic surveys were conducted aiming at detecting eventual archaeological artefacts that could interfere with the future extraction operations. A total field scalar magnetometer G882 (Geometrics, Caesium vapour) was used to acquire data along lines and tie-lines spaced at 50 and 250 m, respectively, at 10 Hz acquisition frequency. The magnetometer was towed with 60 m layback, to avoid noise generated by the vessel (17 m long). Processing of magnetic data included: (1) noise removal; (2) IGRF (International Geomagnetic Reference Field) correction for subtraction of the principal magnetic field; (3) correction of the diurnal anomaly using base station data; (4) iterative data levelling using tie-line intersections; (5) calculation of residual magnetic anomaly by filtering anomalies with wavelengths larger than 500 m; (6) minimum curvature gridding. For the identification of notable anomalies potentially related to archaeological artefacts processing also included: (7) calculation and analysis of the analytic signal (Nabighian 1972) for anomaly enhancement and relocation by shifting to the top of respective causative bodies; and (8) estimation of source depths through Euler deconvolution (Thompson 1982) (structural index SI = 3.0) to identify sources with estimated depths compatible to a location close to the seafloor. The processed data allowed not only identifying possible archaeological artefacts but also investigating for a geological correlation with the other geophysical datasets (Neres *et al.* 2019).

Sand resources assessment methodology

Although the volumes of the various sedimentary units were defined, the employed strategy to calculate the volumes of useful material (coarse sand + medium sand) was based on the individualization of the first 3 m of the sedimentary package in six depth layers of intervals of 50 cm thickness, in which the sediments were characterized and their usability as nourishment material quantified. The sediments that can be employed for nourishment must correspond to classes 1 or 2 (clean and slightly contaminated dredged material), thus eliminating potential impacts due to contamination by POPs and trace metals released from the sand to the water column during dredging operations (Pinto *et al.* 2020). In addition to this, the APA, IP defined a set of extra restrictive specifications to be considered in the estimation of the resource volume: carbonate content <30%, gravel content <15% and the fine fraction (silt + clay) <10%. The volume calculation for each layer was implemented in several calculation steps as described in Figure 2, using Microsoft Excel™ software and the Spatial Analysis and 3D-Analyst extensions of the ESRI ArcGIS™ software. The sediments that respect these specifications are classified as useful sediment. Within the CHIMERA project, the spatial distribution and content of the sum of coarse and medium sand that fulfil all the restrictive specifications was calculated and mapped, thus defining the useful material (Fig. 2). The volumes of useful material were calculated between 0 and 50 cm below seafloor, from 50 to 100 cm, 100 to 150, 150 to 200, 200 to 250 and 250 to 300 cm. The interpolation method used was Inverse Distance Weighted (IDW), with a raster resolution of 10 × 10 m. This method of deterministic (mathematical) spatial interpolation is based on the assumptions that:

- Unsampled point values can be predicted as the weighted average of known values within the vicinity.
- Sampled points closest to the unsampled point are more similar than those farther apart, with the weights inversely proportional to the distances among the forecast locations and the sampled locations.

Results

This article does not intend to show all the results obtained by the CHIMERA project but only a selection of illustrative examples of the distinct types of data obtained and their interpretations, showing the importance of the development of the integrated multidisciplinary approach followed here. This ensures a detailed physical and chemical characterization of the borrow sediments and of their useful volume.

Seafloor morphology and nature

The three northern areas (about 10 km^2 each) are rectangular in shape, oriented parallel to the bathymetric contours, with water depths ranging between 24 and 40 m (Fig. 1). The seafloor presents, in general, as undulations and soft slopes with maximum amplitudes of approximately 25 cm, oriented parallel to the general bathymetry contours. In these areas, only scarce topographic highs were detected, here

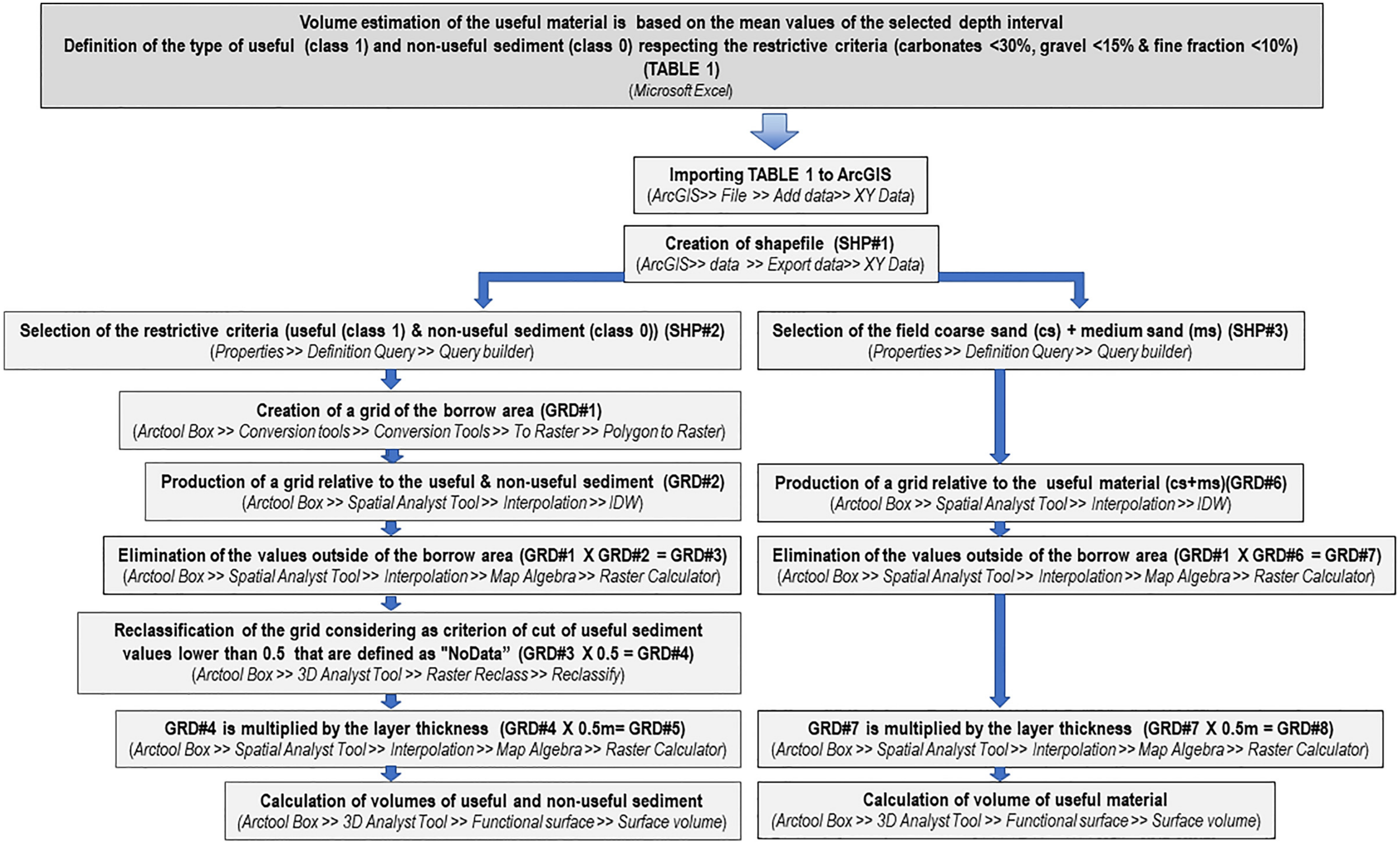

Fig. 2. Volume calculation of useful sediment and useful material (coarse sand + medium sand) workflow conducted in ArcGIS.

defined as ‘sorted bedforms’ (heterogeneous shelf seabed features indicators for hydrodynamic conditions marked by subtle bathymetric reliefs) characterized by decimeter order heights and/or by abrupt variations in grain size. The BM borrow area shows localized reliefs up to 60 cm high in a small zone close to the north limit. The CC borrow area has a near semicircle shape, of approximately 4.9 km^2, located off the coast of Lisbon between depths of 20 and 28 m (Fig. 1) with a general slope of 0.4%. This area presents a set of rippled scour depressions, generally limited by well-defined slopes with maximum amplitudes of the order of 70 cm.

Backscatter intensity and sedimentary characteristics

The backscatter intensity and bathymetric maps together with sedimentological data allowed seafloor sediment distribution patterns to be defined. The backscatter mosaics obtained for the four borrow areas reveal spatial coherent patterns including areas with lower and higher acoustic backscatter intensities. From the analysis of the bathymetric, backscatter and surface samples data, interpreted sediment textural distribution maps were produced for all areas. An example of the 350 kHz multibeam backscatter mosaic obtained in the CC borrow area is shown in Figure 3. The histogram for the backscatter values presents a distribution with a main mode centred around −34 dB and a secondary mode at −24 dB. The main mode (−34 dB) corresponds to the very fine to medium sand, that covers most of the borrow area. Medium to coarse sands were observed in areas with high reflectivity, corresponding to the secondary mode (−24 dB), found in small depressions (areas of maximum slope gradients corresponding to 70 cm depressions of the seafloor) with half-moon (barchan-like) and rounded shapes (Fig. 3).

Surface sediments are mainly composed of sand, with fine fraction (<63 µm) contents lower than 4% in all the borrow areas. The two northernmost borrow areas, ET and BM, are characterized by low spatial variability, with more than 50% of the surface samples showing a mean grain size corresponding to coarse sand (Fig. 4a). The FF and CC borrow areas present the highest particle size variability. The mean grain size varies between fine and very coarse sand (Fig. 4b). In terms of sorting, the ET and BM surface samples show the highest variability (Fig. 4b). The median sorting values for all borrow areas lie in Folk’s moderately sorted category (Fig. 4b). The surface samples have a median gravel content lower than 10% in the four borrow areas

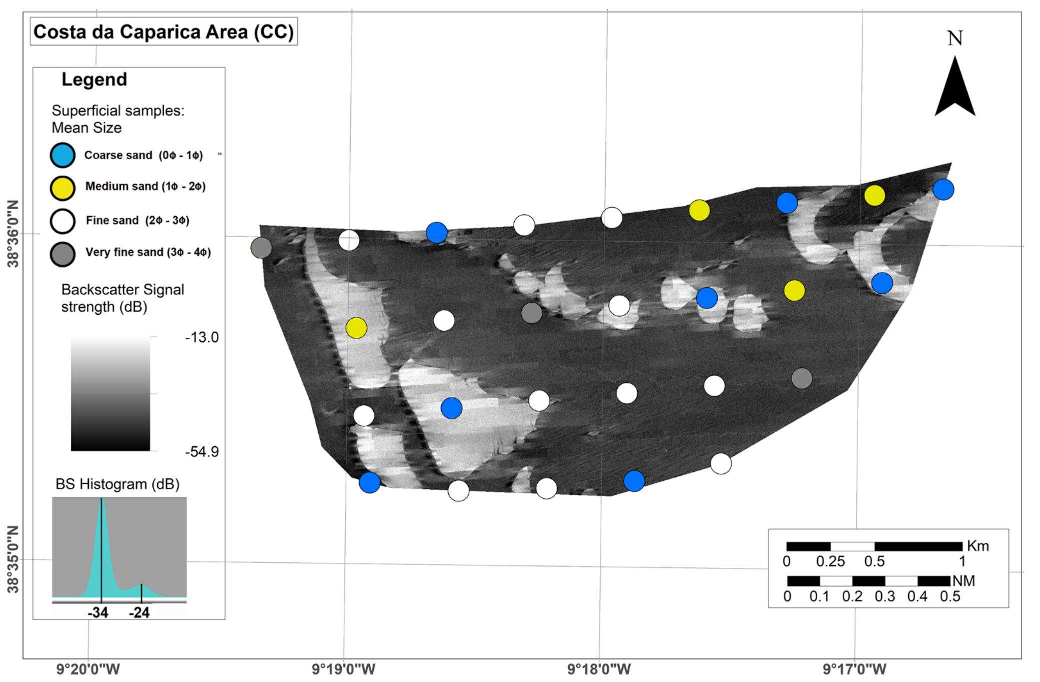

Fig. 3. The 350 kHz multibeam backscatter mosaic of the CC borrow area. Overlapped on the backscatter mosaic are the sediment types identified at each sample location. Inset: backscatter histogram with the two modes.

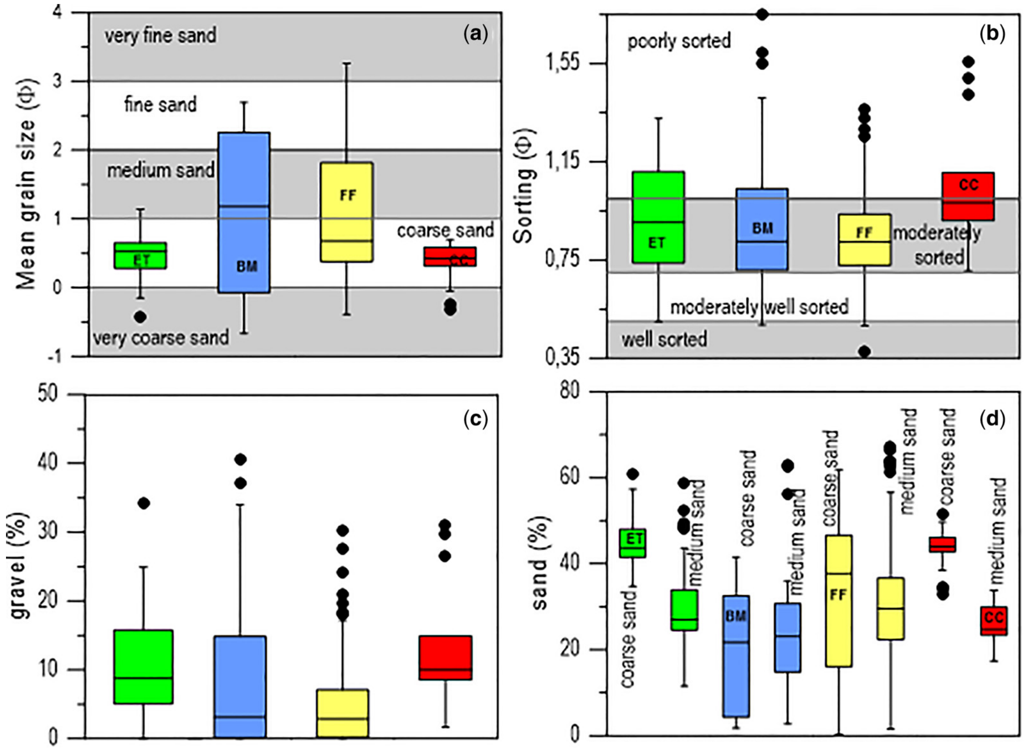

Fig. 4. Box-and-whisker plots representing the Folk and Ward Graphical methods (1957): (**a**) mean grain size; (**b**) sorting; (**c**) gravel; (**d**) coarse and medium sand contents in the four borrow areas. The plots show the minimum, maximum, median and lower and upper quartiles. The boxes represent the interquartile range that contains 50% of the values. The whiskers are the lines that extend from the boxes to the highest and lowest values. The lines across the boxes indicate the median. Outliers (defined as 1.5 × inter-quartile range) are represented by black filled symbols.

(Fig. 4c). The composition of the gravel fraction is dominated by shell debris in the CC borrow area and by quartz grains in the other three areas. The ET and BM borrow areas have the highest median contents of coarse sand, while the FF and CC show high contents of medium sand (Fig. 4d).

Regarding carbonates content, the CC borrow area presents both high variability and the highest median $CaCO_3$ contents (Fig. 5a). The area also presents the greater variability in C_{org} contents and density values (Fig. 5b). Nevertheless, it is important to highlight that the median contents of C_{org} are lower than 0.2%. The total solids content varies between 77 and 94% in all borrow areas, which is consistent with the mostly sandy composition (the median values of the sand fraction in ET, BM, FF and CC borrow areas are 90, 94, 99 and 98%, respectively (Fig. 5c).

A scatterplot of the mean grain size and sorting values from the ET and BM areas evidences that coarse sediments show high sorting values (Fig. 6a & b). This relationship was not observed for the FF and CC borrow areas (Fig. 6c & d).

Characterization of the degree of contamination

The evaluation of the degree of contamination is based on the comparison of the trace metal and POP contents with the ranges of concentrations of the five categories defined by the Portuguese Legislation (Ordinance 1450/2007, 12 November) (Table S1). All the selected surface sediment samples were classified as Class 1.

Subsurface morphosedimentary facies

Seismic interpretation of the deeper layers indicate that this detrital sediment package is present on all four areas up to depths that range between 4.7 and 57.3 m below seafloor (Table 2). This sedimentary package, not affected by tectonic deformation, lies unconformably on a clearly imaged deformed bedrock substrate. The sedimentary architecture of this sediment package was organized in four to six SUs bounded by discontinuities, usually of erosional nature, which were independently defined for each

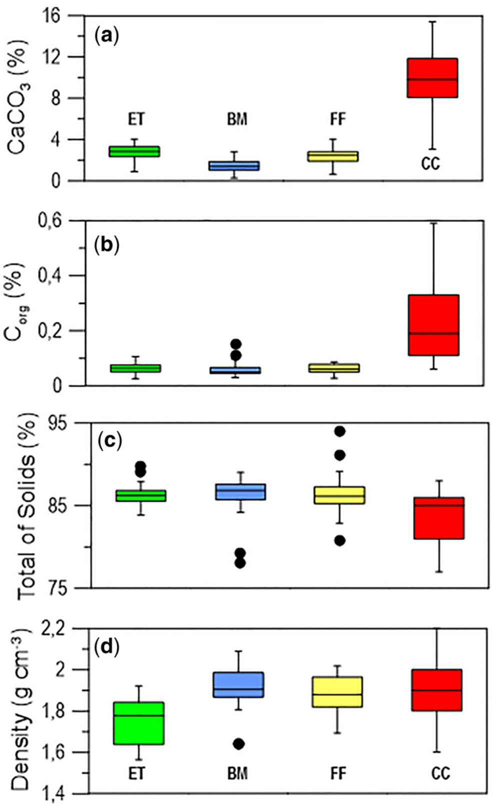

Fig. 5. Box-and-whisker plots representing (**a**) the $CaCO_3$, (**b**) the C_{org} contents, (**c**) the total solids content and (**d**) the density in the surface sediments of the four borrow areas.

project area. The SUs exhibit complex internal geometries and inter-unit arrangements that vary significantly not only across the project areas but also locally inside the same area. However, the spacing defined for the survey grid allowed to image and delineate the 3D geometry of all these sedimentary bodies.

The outcropping SU that tops the sediment packages, being the easiest to mobilize and dredge, has a very similar geometry in all borrow areas. This unit corresponds to a thin sediment layer, 0.2–1.7 m thick, which extends throughout the four studied areas. The exception was found in small sections of FF area, where another SU outcrops. The unconformable base of this upper SU most frequently coincides with the base of sea bottom morphological features (e.g. sorted bedforms or rippled scour depressions). Beneath this superficial unit, lies a sequence of usually thicker sediment packages wherein two types of morphological features stand out, infilled channels and sediment bodies. They are interpreted as former coastal barriers, as already proposed (e.g. Rodrigues *et al.* 1991; Dias *et al.* 2000, 2002).

Infilled channels' features, occasionally showing several successive cycles, are present in the four working areas. The channels' dimensions range from the seismic resolution limit to structures comprehending an entire SU (e.g. unit U6 of area BM) with a length of more than 3500 m, 750 m wide and 30 m of depth. Sometimes these features occur related to the landward side of sediment bodies interpreted as coastal barriers (e.g. units U3 and U4 of area BM). The most prominent sediment bodies associated with former coastal barriers are the ones from the FF and BM areas (units U3, in both areas), reaching thicknesses of more than 8 m, 3750 m of length and 1750 m of width. These features are characterized by high amplitude sigmoidal to oblique downlap, prograding internal reflections that have frequent internal discontinuities and are limited at their top by an erosive unconformity (Figs 7 & 8). They can be remnants of coastal barriers, associated with palaeocoastlines (e.g. delta, swash bar or other shoreface structures,) or detached coastlines structures (e.g. barrier islands system).

Absolute age control of the SU was not undertaken. However, sedimentary architecture and facies similarities with other coastal sectors and neighbouring inland geology, suggest that the bedrock substrate could be of Meso-Cenozoic age (probably Cretaceous to Miocene) and that the generation of the overlaying detrital sequence can be associated with the sea-level variation of the last Quaternary eustatic cycles.

Grain size down-core variability

The vibrocorer samples up to 3 m below seafloor confirmed the quartz rich sand/gravel nature of the upper sediment layers imaged in the PE data, characterized by minor percentages of fine-grained sediments (Fig. 9). The dominant dimensional classes vary among borrow areas (Fig. 9). The two most northern areas (ET and BM) are characterized by coarser sediments compared to the FF and CC borrow areas (Fig. 9). While ET sediments are essentially coarse to very coarse sands, medium to coarse sediments predominate in BM. The CC borrow area is dominated by fine to medium sands. Considering the example of the FF borrow area, the dominant dimensional classes in the sediment vibrocores are fine and medium sands (Fig. 9). The mean grain size and sorting coefficient (Graphical method, Folk and Ward 1957) do not generally exhibit great variability with depth. Some cores (e.g. FF-V_16 and FF-V_17) have a larger amount of coarse sand at the deeper levels. In terms of sorting the sediment samples, they vary mainly between moderately and poorly sorted (Fig. 10).

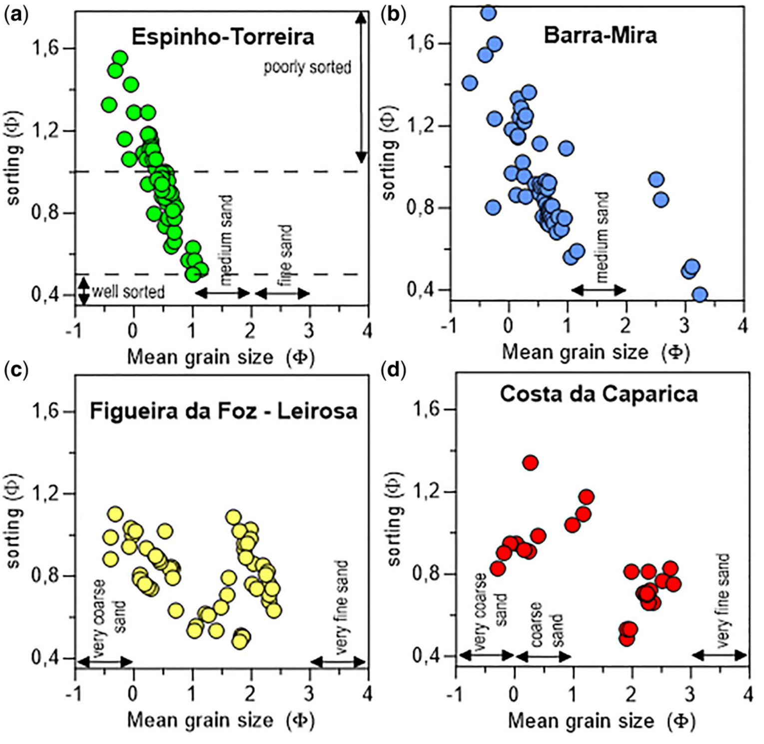

Fig. 6. Mean grain size v. sorting values (Graphical method, Folk and Ward 1957) of the surface samples collected in the four borrow areas: (**a**) ET; (**b**) BM; (**c**) FF; (**d**) CC.

Notable magnetic anomalies / potential archaeological structures

The identification of potential archaeological artefacts either at the seafloor or partially buried was made by analysing each acquired line and the processed grids, residual anomaly and analytic signal, for detecting significant dipolar isolated anomalies. For the identified anomalies, source depth was estimated by Euler deconvolution to check their consistency with depths close to the seafloor. The criteria for defining target anomalies were: local dipole in the residual anomaly verified along line (*c.* 0.5 m resolution) or recorded in more than one line (line separation is 50 m; Figs 11 & 12); maximum analytic signal; and estimated source depth compatible to a location close to the seafloor.

Three target anomalies were identified, one for each borrow area, except FF. The identification of the BM target anomaly is shown in Figure 11. It shows a crop of the BM residual anomaly and the respective analytic signal grid. In the east part of the area, the black circle highlights a dipolar anomaly of 4.6 nT (peak to peak) also coincident with an analytic signal maximum. This target anomaly has an estimated source depth of 27 m below sea-level, compatible with an object buried 1–2 m below seafloor. Given the anomaly wavelength and the survey resolution, the causative body is expected to be less than 100 m long.

Table 2. *Number of upper basements individualized SUs, estimated sediment thickness for the upper basement, volumes for the upper basement and upper SU. The volumes are obtained from depth differencing of the SU horizons*

Area	Number of upper basements SU	Sediment thickness (m)	Sediment volume (10^6 m^3)	
		Upper basement	Upper basement	Upper SU
CC	6	23.4–57.3	230	5.6
BM	6	4.7–15.2	105	9.8
ET	4	7.5–30.9	151	9.3
FF	4	15.8–22.3	183	7.8

Subsurface structure: insight from magnetic data

The total magnetic anomaly showed varying characteristics among the four areas, with amplitudes

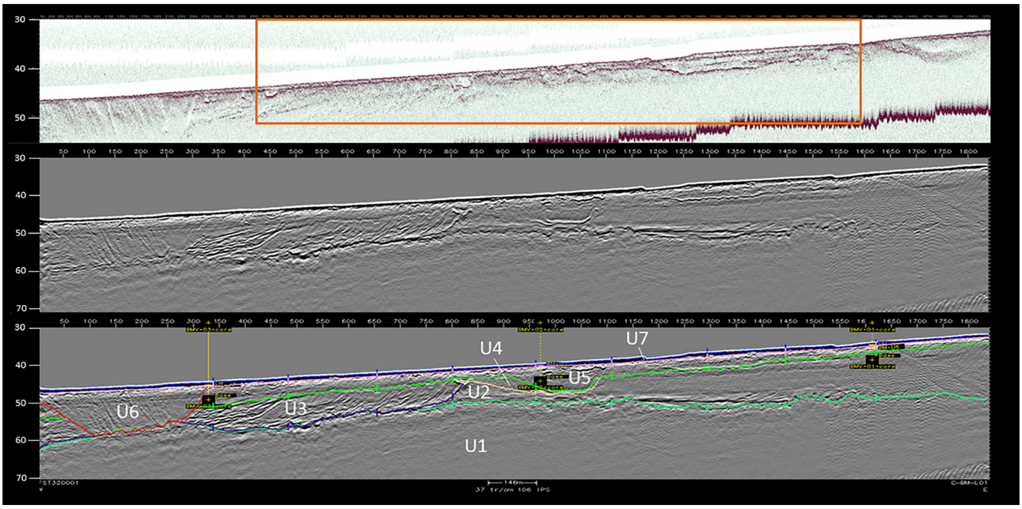

Fig. 7. Line BM_L08, PE (top), UHRS (middle) and UHRS with seismic interpretation and vibrocore sampling data locations superimposed (lower). Orange box outlines the area enlarged in Figure 8.

varying from 12 nT in FF to 200 nT in BM. In general, the total anomaly expresses long wavelength anomalies that are due to the deep geology, not observed in the structure imaged by the high-resolution seismic with shallow penetration (Neres *et al.* 2019). The residual magnetic anomaly is characterized by very low amplitudes: *c.* 2 nT for FF, ET and BM, and *c.* 10 nT for CC. The

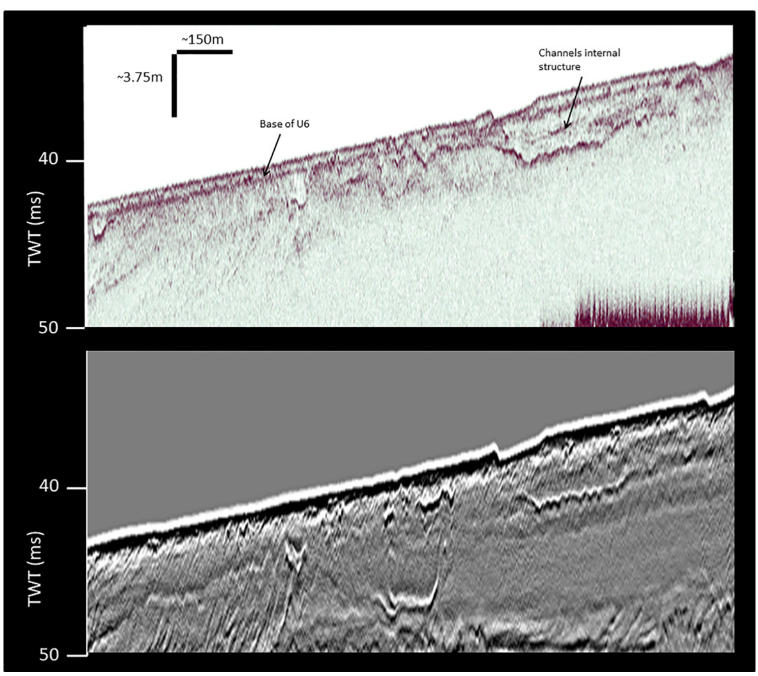

Fig. 8. Detail of PE (top) and UHR (bottom) profiles BM_L01, showing structures hardly imaged in the UHR data. Namely, the base of the upper most unit (U7) and the internal structure of unit U6 channels.

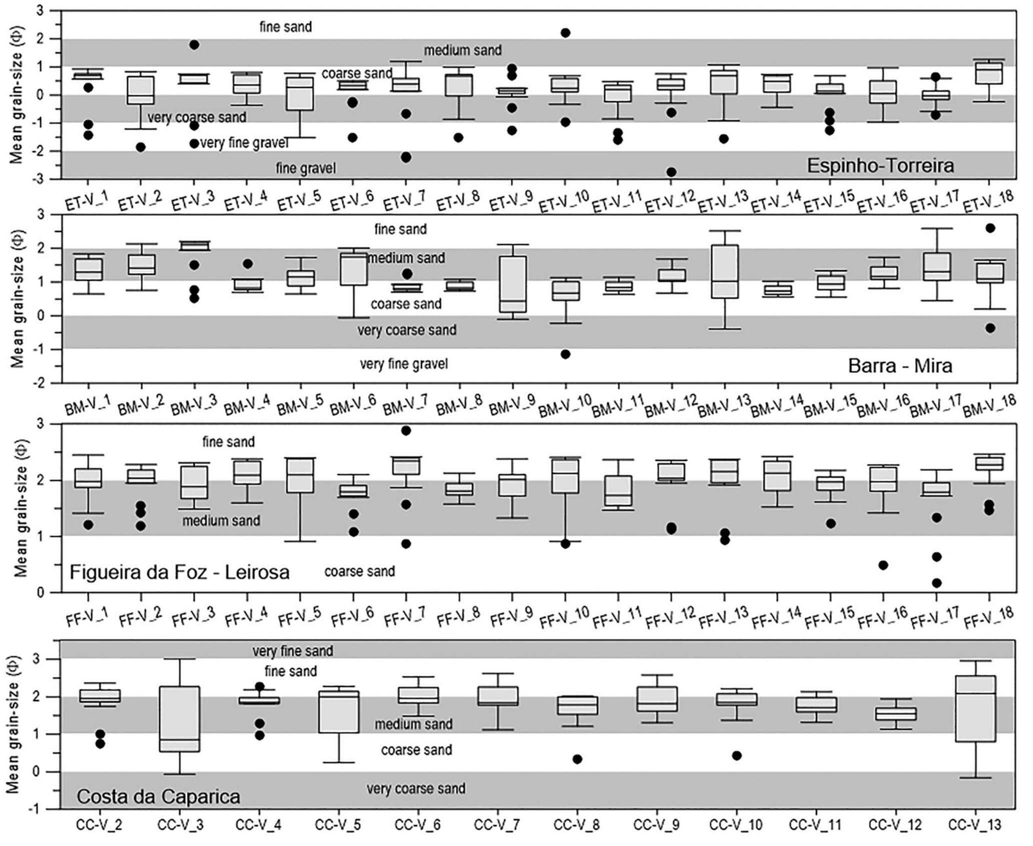

Fig. 9. Box-and-whisker plots representing the mean grain size of the sediments collected in the four borrow areas.

geological significance of the residual anomaly varies among the four study areas. According to the joint analysis with multichannel seismics, it reflects either the intra-basement structure, or some supra-basement sedimentary features such as buried channels and coastal barriers.

The magnetic results and combined analysis for the area ET is illustrated in Figure 11. The gridded total and residual magnetic anomalies, the gridded depth to the top of seismostratigraphic units U1 and U2 and the seismic interpretation of the MCS line X06. Outstanding features in the SUs are the channels in the north of the ET area that cut more than 15 m deep into the basement (marked as # in Fig. 11) and palaeoreliefs rising up to 10 m above the basement at the SW (marked as *). Joint analysis of the residual magnetic anomaly and sedimentary units show an outstanding magnetic signature coincident with the channels and the U2 reliefs. A quantification of magnetic properties is not possible with the available data, but it can be deduced that unit U2 has a higher magnetic susceptibility than U3. This may indicate a more terrigenous sedimentary contribution for U2, and thus a later progression of the coastline to the east. The magnetic signature of the northern palaeochannels may be due to a contrast between the filling sediments and a higher susceptibility basement.

Discussion

Adopted methodology to assess sand resources

Reliable assessment of sand and gravel resources for beach nourishment and the planning of the dredging operations requires the identification and characterization of the sedimentary package and its 3D geometry, as well as the identification and depth distribution of the basement below the sedimentary cover. Only with all this information it is possible to estimate volumes of material that can be dredged for nourishment. This characterization is also important to select and to define the necessary

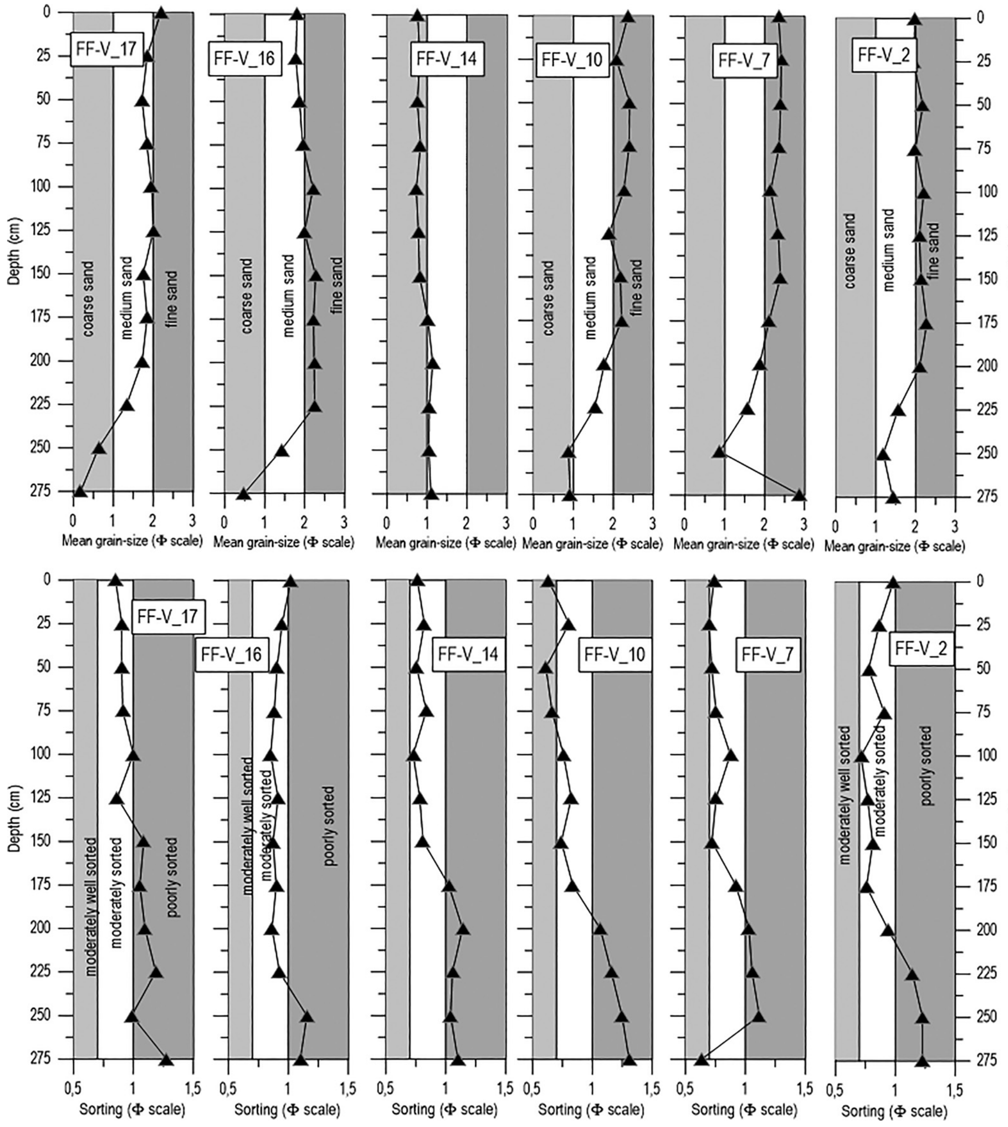

Fig. 10. Mean grain size and sorting (Graphical method) down-core variability in selected sediment cores collected in the FF borrow area.

and more adequate dredging techniques and to identify the potential operation difficulties.

The Portuguese inner continental shelf has a very complex geology, with the record of the interplay between erosion stages during the last glacial maximum and sedimentary infill episodes during transgressions, very frequently sculpted in various glacial–interglacial cycles (Rodrigues *et al.* 1991; Dias *et al.* 2000). The Portuguese inner shelf sedimentary deposits typically include continental meander-like sandy deposits, beach and beach barriers that have migrated according to the transgressive cycles (Rodrigues *et al.* 1991; Dias *et al.* 2000), which are also identified in these four case studies (e.g. Figs 7 & 8). Consequently, the required image and characterization of the sedimentary deposits need to be based on the seafloor characterization by multibeam bathymetry, on the acoustic backscatter and seafloor ground-truthing for sedimentary characterization, and on a dense grid of high-resolution seismic profiles to image the subseafloor geometry of the sedimentary bodies.

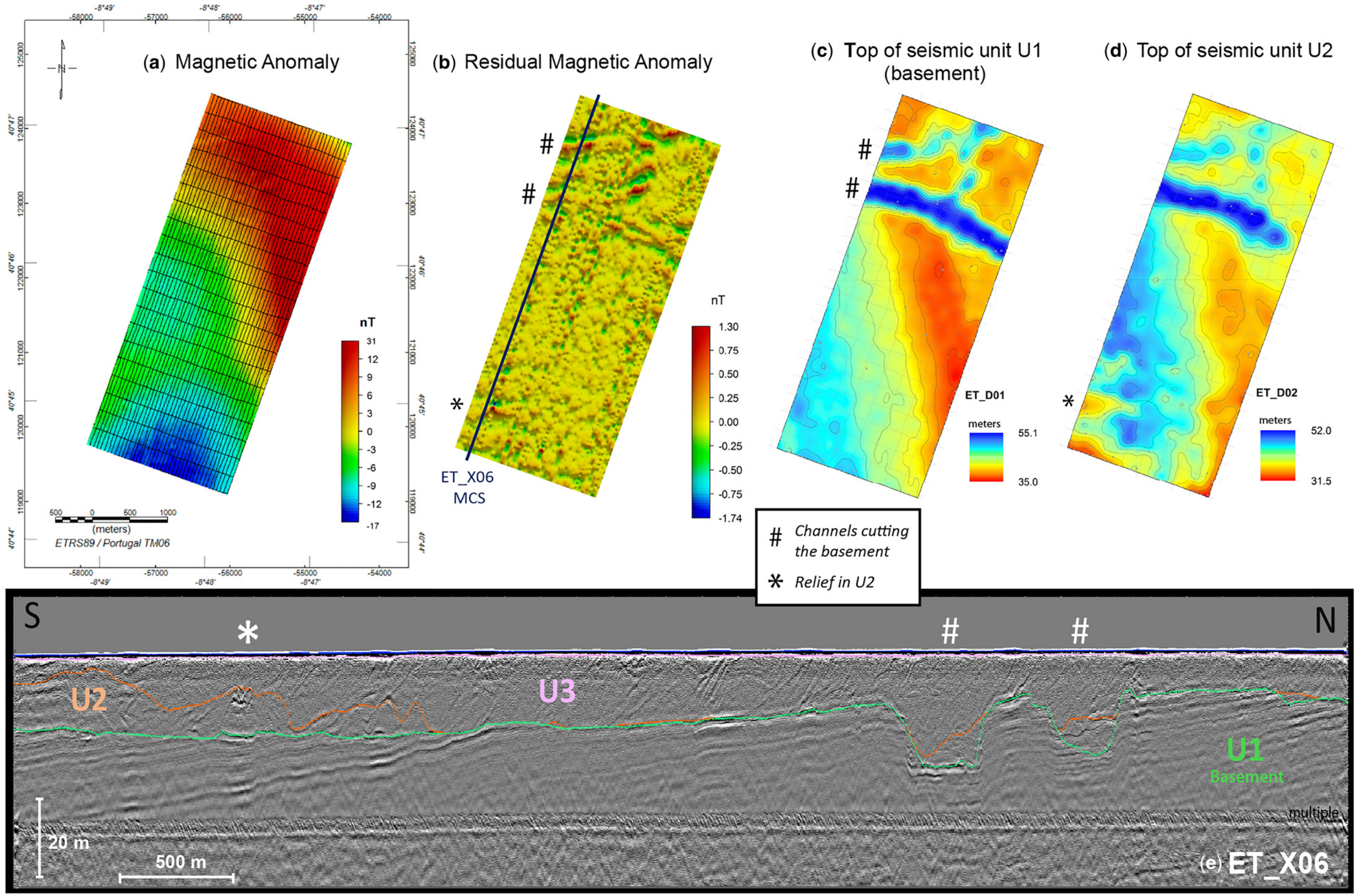

Fig. 11. Magnetic data analysis and relation with identified SUs: example for area ET. (**a**) Total magnetic anomaly grid and survey lines. The high amplitude, long wavelength anomalies are due to regional geology. (**b**) Residual magnetic anomaly grid. The residual magnetic anomaly is marked by low amplitude though outstanding magnetic lineations in the north of the area, and shorter lineations at SW. (**c**) Gridded depth to the top of seismostratigraphic unit U1 (top of basement). (**d**) Gridded depth to the top of seismostratigraphic unit U2. (**e**) Interpretation of the seismic profile X06 (location shown in b). * locates reliefs in unit U2 and # locates channels cutting through the basement and filled by U2 and U3 material.

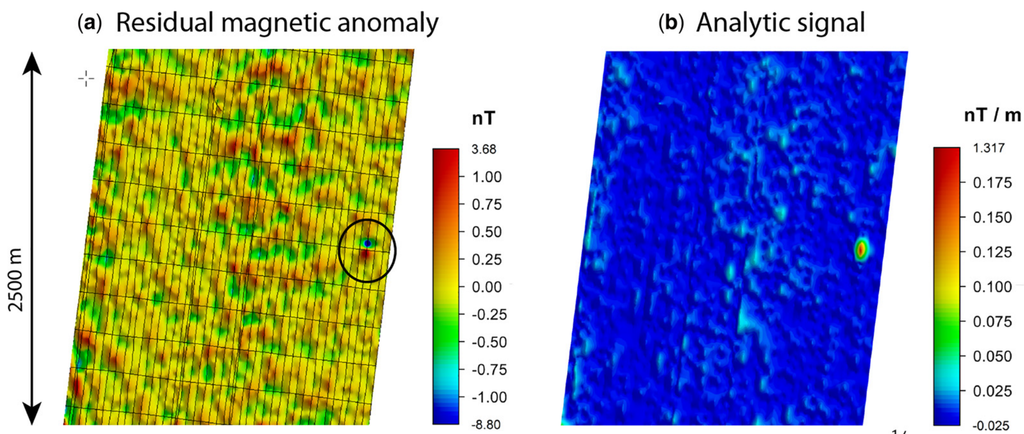

$$as = \left(\left(\frac{\partial T}{\partial x}\right)^2 + \left(\frac{\partial T}{\partial y}\right)^2 + \left(\frac{\partial T}{\partial z}\right)^2\right)^{1/2}$$

Fig. 12. Identification of a magnetic target possibly attributed to an archaeological artefact (example for the area BM). (**a**) Residual magnetic anomaly and survey lines; (**b**) analytic signal. The target anomaly, to the east (black circle), is identified as a local dipole in the residual anomaly and a maximum of analytic signal.

In this work, the adopted methodology to fulfil the objectives included the following steps: (1) mapping the surface bathymetry and backscatter, and correlating the backscatter with the surface samples; (2) acquisition of high resolution seismics to define the Quaternary sedimentary package and SUs within; (3) definition of the sedimentary systems and main units of the Quaternary sedimentary package; (4) quantification of volumes of useful sediment and material content in the top 3 m of the Quaternary package that fulfil all the requirements for use. Thus, the seafloor bathymetry was acquired with full coverage, with more than 10% superposition of parallel swath coverages, ensuring a bathymetric resolution of 25 cm. The dense surface sampling grid allowed the characterization of the nature of the seafloor, in terms of granulometry, $CaCO_3$ contents and chemical characterization. The seafloor ground-truth allowed calibrating the swath backscatter classification and confirmed that the density of the sampling stations was both adequate and what was required to map the seafloor natural variability. Multichannel seismic profiles were acquired with 250 m spacing between parallel lines, ensuring that the basement was imaged and that all the expected geomorphologies in an inner-shelf setting were identified and mapped. The vibrocorer sampling of the top 3 m was done with a grid space of 500 and 1000 m. This 3 m depth was sufficient since this is the expected maximum depth of dredging. The sampling allowed for characterizing the different sedimentary bodies present in the four study areas. Since this project's workflow defined that the vibrocorer sampling was to be done in a regular grid, the number of vertical sampling stations frequently over sampled the same sedimentary body. This allowed confirmation that the sedimentary structures exhibit very little lateral variability in terms of the required properties – granulometry, composition and contamination. The definition of the sedimentary systems and main units of the Quaternary sedimentary package were done by comparing and correlating the seismic stratigraphy with the results of the lithological characterization of the vibrocores, as described in the section below. The definition and quantification of volumes of ‘useful sediment’ and of ‘useful material’ was done for the top 3 m of the Quaternary package in the individual 50 cm thick layers, excluding the volumes of material that did not fulfil the $CaCO_3$,

Table 3. *Volumes in m^3 of non-useful and useful sediment (carbonates <30%, gravel <15% and fine fraction <10%), and useful material, for two sediment layers of the CC borrow area*

Depth Interval	Volume of non-useful sediment	Volume of useful sediment	Volume of useful material (coarse sand + medium sand)
0–50 cm	0.15×10^6	2.30×10^6	0.97×10^6
150–200 cm		2.13×10^6	1.09×10^6

grain-size and contaminants requirements for use as nourishment material.

Comparison of lithologic and seismic stratigraphy

Seismic interpretation of the multichannel high-resolution dataset was done to establish a seismic stratigraphic model of each site, defining units which are characterized by their geometries, external relationships and the internal configuration of reflectors. The depositional context of these SUs was inferred, and the lithological variations of the units was assessed and later confirmed by the vibrocore samples characterization. This methodology allowed to map the base of the Quaternary package in the four borrow areas as defined by the deeper reflectors within the sandy deposits, which reached maximum depths below seafloor of 55.1 (ET), 45.2 (BM), 59.7 (FF) and 84.2 m (CC). However, it is only the complementary correlation of the lithological stratigraphy with the seismic stratigraphy that leads to the inference that the sedimentary facies and the palaeoenvironment correspond to the top (3 m) SUs. In most cases the facies could be extrapolated to deeper parts of the units. In some regions of the four study areas, the fine-scale sedimentary variability was not clearly imaged by the seismic data. But in general, a good correlation between major (metre scale) sedimentary packages and the top seismic reflectors was achieved. Based

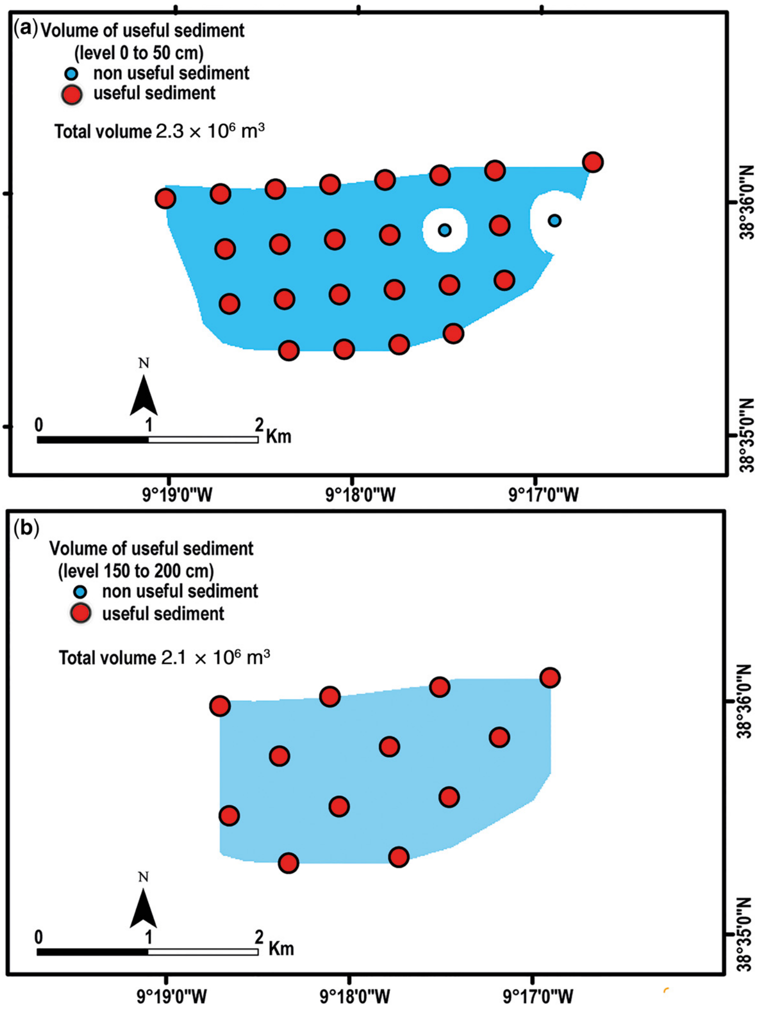

Fig. 13. Spatial distribution maps of the useful sediments volume in the CC area. (**a**) At level 0–50 cm and (**b**) 150–200 cm.

on the composition of the units within the top 3 m and on the geometry and characteristics of the seismic reflectors below the top 3 m, we could infer the sedimentary geometry and the sedimentary settings of these units.

Estimation of sand resources

The case study of the CC borrow area is presented here as an example of the adopted strategy to estimate the sand resources. The methodology implemented in this project is described for two depth intervals: 0–50 and 150–200 cm, and the volumes of useful sediment and useful material are shown in Table 3. In the top layer, two surface samples (blue dots in Fig. 13) with gravel contents higher than 15% do not fulfil the required criteria and were therefore not considered for the calculation of useful sediment volume. In these two examples, it is possible to observe that only 42% (top interval) and 51% (deep interval) of the useful sediment is considered as useful material. This indicates a high abundance of other dimensional classes (e.g. fine sand) in this borrow area. The spatial distribution pattern of useful material varies in depth, with the lowest mean contents being found in the western half of the area for the most recent sediments, while in the sediment layer, 150–200 cm, they were mainly located in the southeastern limit (Fig. 14).

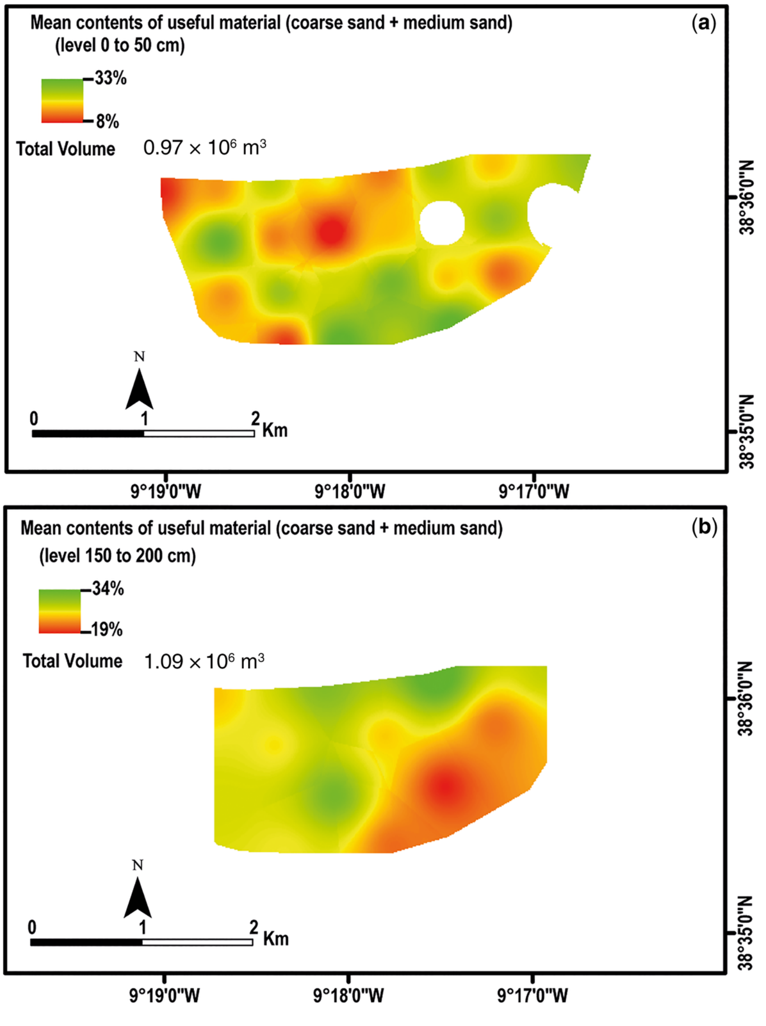

Fig. 14. Spatial distribution maps of the mean contents of useful material (medium sand + coarse sand) and respective volume units in the CC area. (**a**) At level 0–50 cm and (**b**) 150–200 cm.

The results obtained for the four borrow areas confirm the almost generalized existence of useful sediments (fines – silt and clay <10%; gravel <15%; carbonates <30%; no contaminants) dominating the sands dimensional class. For an exploration depth of 3 m, a volume of the order of 14×10^6 m^3 is estimated at ET and CC, and 28×10^6 and 29×10^6 m^3 at the BM and FF spots, respectively. The seismic-stratigraphic model inferred from geophysical data indicates bedrock between 6 and 57 m below the seabed in the four areas.

Sediment management strategy

The sediment management strategy allows for establishing the goals to manage and assure a sustainable exploitation of the sand resources. The results obtained show sedimentary resources (in a thickness of 3 m) compatible with a sediment management strategy based on sediment budget balance until the year of 2035 (ET) and until 2050 (BM, FF and CC), if the nourishment volumes are equal to the magnitude of the residual littoral drift in the reference situation at each site. Furthermore, there is potential to prolong the longevity of the borrow areas, since the sedimentary thickness interpreted on the reflection seismic data suggests the possibility of further increase of the exploration depth and therefore the total volume of useful material.

Final considerations

Offshore sand is a limited resource, whose renewal depends on various natural and anthropogenic environmental variables, the interaction of which can be quite unpredictable. Therefore, offshore sand resources must be properly managed to ensure sustainability of the ongoing shore protection strategy in Portugal – as in other European countries, such as the Netherlands, Denmark, the UK and Spain – based on beach nourishment. The latter aims to minimize or reverse large background erosion in coastal cells with sediment deficit.

The results obtained in this work show suitable sand (in quality and quantity) in the four selected areas, which enable a series of artificial beach nourishment interventions to be undertaken in the medium–long term. The decision process regarding the prioritization of places and type of nourishment, volumes involved and refill periodicity will depend on the results obtained by the business case and environmental impact assessment, but also by financial, political, administrative and social constraints.

Quantification and spatial distribution of both useful sediment volume and sand quality is of great importance for selecting/detailing the area to be dredged. This information is fundamental for management of the sedimentary resources for beach nourishment in areas of intense coastal erosion. Additionally, the detailed textural information on the nourishment material will allow for hydrodynamic modelling and thus prediction of the sustainability of the nourished beaches. Also, the baseline bathymetric and backscatter mapping of the borrow area allows for subsequent evaluation of the morphological evolution of the extraction pits upon implementation of monitoring programmes. One of the aims of the monitoring programmes is to integrate diverse (e.g. hydrodynamic, morphological, sedimentological and biological) information from the borrow and fill areas, during the different phases of the operation.

Both the methodology and the data acquired within the CHIMERA project ensure the understanding of the Quaternary sand deposits as well as its sedimentological characteristics, geometry and degree of contamination. This information is essential to assess the suitability of the deposits for beach nourishment. They also allow for identifying possible archaeological artefacts that might interfere with the future dredging operations. The quantification and mapping of the 3D sub-surface distribution of the useful sediment material was designed to guarantee selection of the appropriate dredging operations in these inner shelves complex systems with large spatial variability. The detailed characterization of the borrow site sediments allowed identification and selection of the most suitable useful material.

Acknowledgements The authors are grateful to António Pereira, Cremilde Monteiro, Cristina Micaelo, Rui Silva, Rute Granja and Warley Soares for helping in the laboratory work. Special acknowledgments are due to the diving team of the Xavisub Lda for the high-quality sediment sampling operations. The authors also thank the company Geosurveys Geophysical Consultants Ltd, for providing the flow template used in this work for processing the UHRS data and the EMSO-PT project (ref. PINFRA/22157/2016).

Funding The CHIMERA project was funded by the Agência Portuguesa do Ambiente and European Comission through the Operational Programme for Sustainability and Efficiency in the Use of Resources (POSEUR-09-2016-48-FC-000030). Emília Salgueiro and Marta Neres were funded by postdoctoral FCT fellowships: SFRH/BPD/111433/2015 and SFRH/BPD/96829/2013, respectively.

Author contributions **MMH**: investigation (lead), project administration (lead), resources (lead), supervision (lead), validation (lead), writing – review & editing (lead); **PB**: investigation (lead), methodology (lead), writing – review & editing (equal); **VM**: writing – original draft (lead), writing – review & editing (lead); **MR**: investigation (equal), methodology (lead), writing – review &

editing (equal); **MN**: investigation (lead), methodology (lead), writing – review & editing (equal); **MS**: investigation (equal), methodology (equal), validation (equal); **ES**: investigation (equal), methodology (equal), writing – review & editing (supporting); **TD**: investigation (equal), methodology (equal), writing – review & editing (supporting); **AIR**: investigation (equal), methodology (equal), writing – review & editing (supporting); **MTG**: investigation (lead), methodology (lead), writing – review & editing (equal); **MJG**: investigation (equal), methodology (equal), validation (lead), writing – review & editing (supporting); **EA**: investigation (equal), methodology (equal); **MS**: investigation (equal), methodology (equal); **MF**: investigation (equal), methodology (equal); **CAP**: writing – review & editing (equal); **CB**: investigation (equal), methodology (equal); **PT**: investigation (equal), methodology (equal), project administration (lead), writing – review & editing (lead).

Data availability statement The datasets generated during the current study are not publicly available due to confidentiality agreements with research collaborators. Data are however available from the authors upon reasonable request and with permission of the Núcleo de Monitorização Costeira e Risco – Agência Portuguesa do Ambiente.

References

Andrade, C., Freitas, M.C., Cachado, C., Cardoso, A., Monteiro, J., Brito, P. and Rebelo, L. 2002. Coastal zones. *In*: Santos, F.D., Forbes, K. and Moita, R. (eds) *Climate Change in Portugal: Scenarios, Impacts and Adaptation Measures*. Gradiva.

Andrade, C., Rodrigues, A. *et al*. 2015. *Gestão da Zona Costeira O Desafio da Mudança*. Sediment Working Group: Final report, http://www.apambiente.pt/_zdata/DESTAQUES/2015/GTL_Relatorio%20Final_20150416.pdf [in Portuguese].

Anthony, E.J., Cohen, O. and Sabatier, F. 2011. Chronic offshore loss of nourishment on Nice beach, French Riviera: a case of over-nourishment of a steep beach? *Coastal Engineering*, **58**, 374–383, https://doi.org/10.1016/j.coastaleng.2010.11.001

Blott, S.J. and Pye, K. 2001. Gradistat: A grain size distribution and statistics package for the analysis of unconsolidated sediments. Earth Surf. Process. *Landforms*, **26**, 1237–1248, https://doi.org/10.1002/esp.261.

Costley, C.T., Mossop, K.F., Dean, J.R., Garden, L.M., Marshall, J. and Carroll, J. 2000. Determination of mercury in environmental and biological samples using pyrolysis atomic absorption spectrometry with gold amalgamation. *Analytica Chimica Acta*, **405**, 179–183, https://doi.org/10.1016/S0003-2670(99)00742-4

Davis, R.A., Jr, Wang, P. and Silverman, B.R. 2000. Comparison of the performance of three adjacent and differently constructed beach nourishment projects on the Gulf Peninsula of Florida. *Journal of Coastal Research*, **16**, 396–407.

Dias, J.M.A. and Neal, W.J. 1990. Modal size classification of sands: an example from the Northern Portugal Continental-Shelf. *Journal of Sedimentary Petrology*, **60**, 426–437.

Dias, J.M.A. and Nittrouer, C.A. 1984. Continental-shelf sediments of northern Portugal. *Continental Shelf Research*, **3**, 147–165 https://doi.org/10.1016/0278-4343(84)90004-9

Dias, J.M.A., Boski, T., Rodrigues, A. and Magalhães, F. 2000. Coastline evolution in Portugal since the Last Glacial Maximum until present: a synthesis. *Marine Geology*, **170**, 177–186, https://doi.org/10.1016/S0025-3227(00)00073-6

Dias, J.M.A., Jouanneau, J.M. *et al*. 2002. Present day sedimentary processes on the northern Iberian shelf. *Progress in Oceanography*, **52**, 249–259, https://doi.org/10.1016/S0079-6611(02)00009-5

Dondurur, D. 2018. *Acquisition and Processing of Marine Seismic Data*. Elsevier.

Duarte, H., Wardell, N. and Monrigal, O. 2017. Advanced processing for UHR3D shallow marine seismic surveys. *Near Surface Geophysics*, **15**, 347–358, https://doi.org/10.3997/1873-0604.2017022

Ferreira, Ó. and Matias, A. 2013. Portugal. *In*: Pranzini, E. and Williams, A. (eds) *Coastal Erosion and Protection in Europe*. Routledge, 275–293.

Flemming, B.W. and Delafontaine, M.T. 2000. Mass physical properties of muddy intertidal sediments: some applications, misapplications and non-applications. *Continental Shelf Research*, **20**, 1179–1197, https://doi.org/10.1016/S0278-4343(00)00018-2

Folk, R.L. and Ward, W.C. 1957. A study in the significance of grain-size parameters. *Journal of Sedimentary Petrology*, **27**, 3–26, https://doi.org/10.1306/74D70646-2B21-11D7-8648000102C1865D

Friedman, G.M. 1961. Distinction between dune, beach and river sands from their textural characteristics. *Journal of Sedimentary Petrology*, **31**, 514–529.

Hamm, L., Capobianco, M., Dette, H.H., Lechuga, A., Spanhoff, R. and Stive, M.J.F. 2002. A summary of European experience with shore nourishment. *Coastal Engineering*, **47**, 237–264, https://doi.org/10.1016/S0378-3839(02)00127-8

ICES 2016. *Effects of extraction of marine sediments on the marine environment 2005–2011*. ICES Cooperative Research Report No. **330**.

Mougenot, D. 1988. *Geologie de la Marge Portugaise*. PhD Thesis, Université Pierre et Marie Curie Paris VI, France.

Nabighian, M. 1972. The analytic signal of two-dimensional magnetic bodies with polygonal cross-section: its properties and use for automated anomaly interpretation. *Geophysics*, **37**, 507–517, https://doi.org/10.1190/1.1440276

Neres, M., Brito, P. *et al*. 2019. Combining magnetic and seismic reflection data for characterization of inner shelf sand nourishment areas. *Geophysical Research Abstracts*, **21**, EGU2019-4339.

Oliveira, I.M., Valle, A.F. and Miranda, F. 1982. Littoral problems in the Portuguese west coast. *Cape Town, Republic of South Africa, Coastal Eng. 1982 Proceedings, III, 1951–1969.*

Payton, C.E. 1977. Seismic stratigraphy: applications to hydrocarbon exploration. *Memoir of the American Association of Petroleum Geologist*, **26**, 516.

Pinto, C.A., Silveira, T.M. and Teixeira, S.B. 2020. Beach nourishment practice in mainland Portugal (1950–

2017): Overview and retrospective. *Ocean Coast. Manag*. 192, 105211, https://doi.org/10.1016/j.ocecoaman.2020.105211

Rodrigues, A., Magalhães, F. and Dias, J.A. 1991. Evolution of the North Portuguese coast in the last 18,000 years. *Quaternary International*, **9**, 67–74. https://doi.org/10.1016/1040-6182(91)90065-V

Taborda, R. and Andrade, C. 2014. *Morfodinâmica do estuário exterior do Tejo e intervenção na região da Caparica – v1*. Contribution to the Littoral Working Group. **Anex I**, 161–179.

Taborda, R., Freire de Andrade, C. *et al*. 2014. Modelo de circulação sedimentar litoral no arco Caparica-Espichel. *Comunicações Geológicas*, **101**, 641–644.

Thompson, D.T. 1982. EULDPH: a new technique for making computer-assisted depth estimates from magnetic data. *Geophysics*, **47**, 31–37, https://doi.org/10.1190/1.1441278

Udden, J.A. 1914. Mechanical composition of clastic sediments. *Bulletin of the Geological Society of America*, **25**, 655–744, https://doi.org/10.1130/GSAB-25-655

US AID 2009. *Adaptation to Coastal Climate Change: A guidebook for development planners*. US Agency for International Development (US AID).

US EPA 1996. Method 3050B: Acid Digestion of Sediments, Sludges, and Soils, Revision 2. US EPA, Washington, DC.

Van Lancker, V., Francken, F. *et al*. 2017. Building a 4D voxel-based decision support system for a sustainable management of marine geological resources. *In*: Diviacco, P., Leadbetter, A. and Glaves, H. (eds) *Oceanographic and Marine Cross-Domain Data Management for Sustainable Development*. IGI Global, 224–252.

Vera-Cruz, D. 1972. Artificial nourishment of Copacabana beach. *Proceedings 13th Coastal Engineering Conference*. New York: ASCE, 141–163.

Vicente, C. and Clímaco, M. 2012. Trecho de costa do Douro ao cabo Mondego: caracterização geral do processo erosivo. LNEC, relatório 253/2012 – DHA/NEC [abstract in English], http://repositorio.lnec.pt:8080/xmlui/handle/123456789/1004065

Wentworth, C. 1922. A scale of grade and class terms for clastic sediments. *The Journal of Geology*, **30**: 377–392, https://doi.org/10.1086/622910